Dovepress
Taylor & Francis Group

ORIGINAL RESEARCH

Modified Xi-Jiao-Di-Huang Decoction Alleviates Sepsis via Regulating Macrophage Polarization by Inhibiting the PIM2/NF-κB Pathway

Fan Ge[1],*, Fang Tian [2],*, Yeyan Zhu[1], Qixiang Yan[1], Qimeng Sun[1], Jun Lu[1]

[1]Department of Intensive Care Medicine, Affiliated Hospital of Nanjing University of Chinese Medicine, Nanjing, People's Republic of China; [2]Department of Central Laboratory, Affiliated Hospital of Nanjing University of Chinese Medicine, Nanjing, People's Republic of China

*These authors contributed equally to this work

Correspondence: Jun Lu, Department of Intensive Care Medicine, Affiliated Hospital of Nanjing University of Chinese Medicine, Jiangsu Province Hospital of Chinese Medicine, No. 155 Hanzhong Road, Nanjing, Jiangsu Province, 210029, People's Republic of China, Tel + 8613813865758, Email lujun@njucm.edu.cn

Purpose: Modified Xi-Jiao-Di-Huang decoction (MXJDH) has significant clinical efficacy for the treatment of sepsis; however, its mechanism of action remains unclear. The purpose of this study was to investigate the protective effects of MXJDH in septic mice and explore its mechanism of action.

Methods: Utilizing UPLC-Q-TOF-MS, we identified the primary constituents of the compound MXJDH. Subsequently, we created a mouse model for sepsis, observing their overall condition, including specific symptoms and behavior. We also monitored key inflammatory markers and pathological changes in their organs. Flow cytometry was then employed to assess the polarization of macrophages. Transcriptome sequencing was used to identify genes with altered expression patterns. We investigated the connection between MXJDH and the Pim2/NF-κB signaling pathway, a crucial regulatory mechanism in inflammation. Finally, we examined the expression and tissue distribution of macrophages in the sepsis-induced mice.

Results: MXJDH effectively reduces inflammation in sepsis mice, leading to a progressive recovery of organ functions. Moreover, MXJDH facilitates the conversion of macrophages from pro-inflammatory M1 phenotype to anti-inflammatory M2 phenotype. This transformation is potentially mediated through the Pim2/NF-κB signaling pathway. By suppressing Pim2 expression, MXJDH mitigates the nuclear translocation of NF-κB, thereby modulating the expression of downstream inflammatory mediators. The role of MXJDH in regulating macrophage polarization has also been confirmed in sepsis mouse tissues.

Conclusion: MXJDH regulates macrophage polarization, inhibits CRS, and alleviates sepsis by inhibiting the Pim2/NF-κB signaling pathway.

Keywords: modified Xi-Jiao-Di-Huang decoction, sepsis, macrophage polarization, PIM2/NF-κB pathway

Introduction

Sepsis is a life-threatening organ dysfunction caused by a dysregulated host response to infection, and is one of the main causes of death in Intensive Care Unit.[1] Although efforts have been made to improve the treatment of sepsis over the past few years, the incidence and mortality associated with sepsis are still increasing. We still lack a specific molecular therapy for this condition, other than antimicrobial therapy.[2,3] Moreover, long-term, high-dose antibiotic use may cause problems, such as drug resistance and lack of specificity.[4] Therefore, it is essential to develop effective strategies for the treatment of sepsis in a new way. Traditional Chinese medicine plays a significant role in inhibiting inflammatory responses and improving prognosis.

In Traditional Chinese Medicine, sepsis is understood to be caused by an imbalance involving heat, toxin, and stasis. Building upon this foundation, the esteemed Chinese medicine practitioner Mr. Zhou Zhongying introduced the concept of "benefiting Qi and nourishing Yin", highlighting the significance of simultaneously enhancing Qi and replenishing Yin

5017

in the treatment of sepsis. The modified Xi-Jiao-Di-Huang decoction (MXJDH) consists of Cornu Bubali.(Shuiniujiao), Radix Rehmanniae.(Dihuang), Radix Paeoniae Rubra.(Chishao), Cortex Moutan.(Mudanpi), and Coptis chinensis Franch.(Huanglian), Ophiopogon japonicus (L. f). Ker Gawl.(Maidong), and Scrophularia ningpoensis (Hemsl. (Xuanshen), Rheum palmatum L.(Dahuang), Glycyrrhiza uralensis Fisch.(Gancao). Detailed information regarding the herbal composition and medicinal parts of MXJDH is presented in Table 1. The Xi-Jiao-Di-Huang decoction is a classical prescription of traditional Chinese medicine, which clears heat, releases toxicity, and eliminates stasis. On this basis, MXJDH added herbs to benefit Qi and nourish Yin. Clinical practice has shown that it can alleviate inflammatory responses; however, the mechanisms and functional targets of MXJDH remain unclear.

Proviral integration site 2 (Pim2), which exhibits serine/threonine kinase activity, is a protein coding gene. Pim2 is closely associated with cancer. Recent studies have found that Pim2 may be involved in the NF-κB signaling pathway, but research in this area is still relatively limited.[5–7] The NF-κB signaling pathway is a key factor in regulating macrophage polarization. It primarily promotes the polarization of M1 macrophages and indirectly affects the phenotype of M2 macrophages through the expression of pro-inflammatory factors, metabolic reprogramming, and interactions with other signaling pathways.[8,9] So, whether the mechanism of MXJDH in treating sepsis is related to the Pim2/NF-κB signaling pathway, and whether it functions by regulating the polarization state of macrophages. In this study, we explored the mechanism of action of MXJDH and reported a potential novel treatment for sepsis.

Materials and Methods
Reagents
NF-κB-p65 Antibody (Cat No. 21014), NF-κB p65 Mouse Monoclonal Antibody (Cat No. 38054), PIM2 Rabbit mAb (Cat No. 56914), IL10 Antibody (Cat No. 38392), and goat anti-rabbit IgG Secondary Antibody (Cat No. L3012) were purchased from Signalway Antibodies (Jiangsu, China). Beta-actin rabbit polyclonal antibody (Cat No. 20536-1-AP), PIM2 rabbit polyclonal antibody (Cat No. 25865-1-AP), IL-6 rabbit polyclonal antibody (Cat No. 21865-1-AP), and TNF-α rabbit polyclonal antibody (Cat No. 26162-1-AP) were purchased from Proteintech Biocompany (Hubei, China). F4/80 Rabbit pAB (Cat AFW18637) was obtained from AiFang biological (Hunan, China). The FITC Rat Anti-Mouse CD86 antibody (Cat 561962) was purchased from BD Biosciences (Franklin Lakes, NJ, USA). PE anti-mouse CD206 (Cat 141705) was obtained from BioLegend (San Diego, CA, USA). Flow cytometry fixation buffer (Cat. PF00016), and Flow Cytometry Perm Buffer (Cat. PF00017) were purchased from Proteintech (Hubei, China). Lipopolysaccharide (LPS) (CAS 297–473-0) and the CCK-8 Kit (BS350B) were purchased from Biosharp (Guangdong, China). RIPA Lysis buffer (CAT PC101 LOT 017A1203) was obtained from Yamei (Shanghai, China). The Mouse IL-6 ELISA Kit (CAT: FMS-ELM006) was purchased from Fcmacs (Jiangsu, China). The Mouse IL-10 ELISA Kit (CAT. NO JYM0005Mo) was purchased from ABclonal (Hubei, China). The Mouse TNF-α ELISA Kit (CAT: MM-0132M1) was purchased from MEIMIAN (Jiangsu, China). Dexamethasone (CAT. NO GC40775), AZD1208 (CAT. NO GC12660) were obtained from GLPBIO (Montclair, USA). A bicinchoninic acid (BCA) protein assay kit (CAT NO. P0010S) were obtained from Beyotime Biotechnology (Shanghai, China). The nuclear and cytoplasmic protein extraction kits were purchased from

Table 1 Detailed Information of Herbs in MXJDH

Chinese Name	Latin Name	Part(s) Used	Amount (g)
Shuiniujiao	Cornu Bubali.	Horn	30
Dihuang	Radix Rehmanniae.	Roots	24
Chishao	Radix Paeoniae Rubra.	Roots	12
Mudanpi	Cortex Moutan.	Roots	9
Huanglian	Coptis chinensis Franch.	Roots	4
Maidong	Ophiopogon japonicus (L. f.) Ker Gawl.	Roots	6
Xuanshen	Scrophularia ningpoensis Hemsl.	Roots	4
Dahuang	Rheum palmatum L.	Roots and rhizomes	12
Gancao	Glycyrrhiza uralensis Fisch.	Roots and rhizomes	6

Beyotime (Shanghai, China). The RProtein A/G IP/Co-IP Kit (CAT: 36421ES40) was obtained from Yeasen (Shanghai, China). Gallic acid, coptisine chloride, epiberberine, palmatine, and jatrorrhizine hydrochloride standards were purchased from Preferred Biotechnology (Sichuan, China). Harpagide, harpagoside, berberine, chrysophanol, and protocatechuic acid were purchased from HerbPurify (Sichuan, China). Ellagic acid (EA) was purchased from PUSH Biotechnology (Sichuan, China). Liquiritin and ammonium glycyrrhizinate were purchased from FIFDC (Beijing, China).

Preparation of MXJDH Decoction

The herbal raw materials listed in Table 1 were provided by the Jiangsu Province Hospital of Chinese Medicine (Jiangsu, China). The quality of the drugs is controllable (presented in Supplementary Table 1). MXJDH decoction was prepared according to ancient documents. All the herbs were soaked in distilled water for 1 h. Shuiniujiao was decocted earlier on strong fire for 30 min, after which the remaining herbs, except Dahuang, continued to be decocted for 15 min. The sample was subjected to a mild fire and boiled for 40 min. Dahuang was decoctioned for 5 min. The liquid was filtered and set aside. The herbs were then boiled in a strong fire for 15 min, simmered in a mild fire for 20 min, and filtered. The resulting liquids from the two times were combined, concentrated, and set aside at 4 °C. The dose administered to mice was converted according to the dose used in the clinic. The clinical dose of drug 1.53 g/kg (107g/70 kg) used in humans was converted to about 13.92 g/kg in mice, with a proportion of 9.1 times. This dose was used as the high dose for subsequent experiments.

UPLC-Q-TOF-MS Analysis

The main components of MXJDH were determined using an AB SCIEX Triple TOFTM 5600 mass spectrometer (AB Sciex, USA), LC-20A rapid liquid chromatograph (Shimadzu, Japan), and a Thermo AcclaimTM RSLC 120 C18 column (3.0 mm×100 mm, 2.2 μm). The column temperature was 40 °C; mobile phase A was 0.1% formic acid water (v/v), and mobile phase B was acetonitrile. Gradient elution procedure was as follows: 0–3 min, 10%B; 3–20 min, 10–25%B; 20–30 min, 25–40%B; 30–41 min, 40–60%B; 41–55 min, 60–85%B; 55–58 min, 85–95%B; 58–63 min, 95%-100%B. Sample intake capacity was 30 μL at 0.3 mL/min. The Mass spectrometry was performed in both positive and negative ionization modes with the following parameters: temperature, 550°C; curation gas (CUR), 40 psi; ion source GS1, 55 psi; GS2, 55 psi; ion spray voltage (IS), 5500 V/-5500 V; scan range, m/z 50–1500. The ion flow diagrams of MXJDH and the mixed control in positive and negative ionization modes are shown in Figure 1A–D). The LC-MS data for chemical composition analysis LC-MS data for MXJDH are listed in Supplementary Table 2.

Animal Models

This animal study was approved by the Animal Ethics Committee of the Affiliated Hospital of Nanjing University of Traditional Chinese Medicine on October 31, 2020 (Approval No. 2020DW-24-01). Thirty male C57BL/6J mice (6weeks, 20±2 g) were purchased from Annuokang Biological Company (Jiangsu, China) and were kept in the ordinary environment of the animal room of Jiangsu Province Hospital of Chinese Medicine, at a temperature of 20–25 °C, relative humidity of 55%-65%, artificial light and dark time alternating for 12 h, free feeding and drinking, changing the bedding once every three days, and starting the experiment after 3 days of adaptation. Mice were randomly divided into five groups with 6 in each: control group (Control), model group (Model), MXJDH low-dose group (MXJDH-L, 4.64 g/kg), MXJDH middle-dose group (MXJDH-M, 9.28 g/kg) and MXJDH high-dose group (MXJDH-H, 13.92 g/kg). The gavage dose in mice was calculated based on the clinical dose conversion. There was no significant difference in the initial basal body weights between the groups. MXJDH-L, MXJDH-M, and MXJDH-H were intraperitoneally injected with LPS (15 mL·kg-1) to establish a sepsis model.[10] After 0.5 hours, the treatment group was intragastrically administered MXJDH, while the Control and Model groups were administered the same volume of 0.9% saline with a volume of 10 mL·kg-1, and then every 12 h for 60 h. The weight and death of the mice were monitored throughout the entire process, and the body weight was measured every 12 h. The flowchart is shown in Figure 2A. After the experiment, the blood, heart, lung, liver, kidney, small intestine, and peritoneal macrophages of the mice were collected for follow-up experiments.
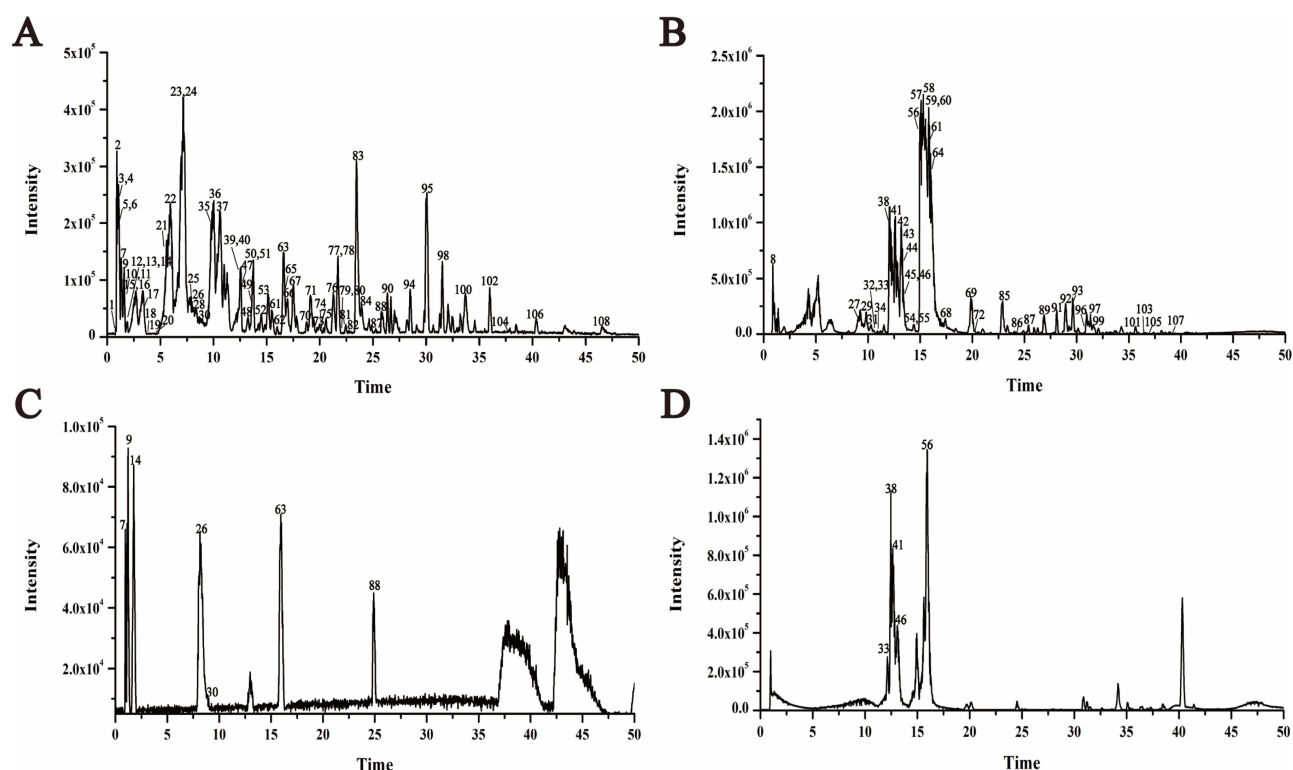
Figure 1 The base peak ion chromatogram of MXJDH and the total ion chromatogram of the mixed reference solution. (**A**) Baseline peak chromatogram (BPC) of MXJDH in negative ion mode. (**B**) Baseline peak chromatogram (BPC) of MXJDH in positive ion mode. (**C**) Total ion chromatogram (TIC) of the mixed control solution in negative ion mode. (**D**) Total ion chromatogram (TIC) of the mixed control solution in positive ion mode.

Blood Routine Examination

Blood was collected from the mice using EDTA anticoagulant tubes, and the white blood cell count, neutrophil percentage, and lymphocyte percentage were detected using a hematology analyzer (Mindray, BC-1800).

Enzyme-Linked Immunosorbent Assay (ELISA)

Mice serum and cell supernatant were collected, and cytokine levels were measured using mouse interleukin (IL)-6, IL-10, and tumor necrosis factor (TNF)-α ELISA kits, according to the manufacturer's instructions.

Haematoxylin and Eosin (HE) Staining

The heart, lung, liver, kidney, and small intestine of mice were fixed with paraformaldehyde and embedded in paraffin. The tissues were cut into 3 μm thick sections and stained for HE for histopathological analysis. Finally, a DS-Qi2 Upright fluorescence microscope (Nikon, Japan) was used to analyze the slices.

Cell Culture, Model Establishment and Intervention

Mouse RAW264.7 macrophages (purchased from Cell Biotech Co.,Ltd (Guangzhou, China)) were cultured in a cell incubator at 37 °C and 5% CO2 for 24 h in DMEM medium containing 10% foetal bovine serum. The cells in the control group were cultured in DMEM without any intervention. The model group was treated with LPS (1 μg/mL) for 24 hours.[11] In the treatment group, MXJDH (50, 100, and 150 μg/mL), Dexamethasone (1μM),[12] AZD1208 (1μM)[13] were added after 3 h of LPS (1 μg/mL) treatment for 21 h. After the above intervention, the cells were used for follow-up experiments.

Cell Viability

RAW264.7 cells were seeded into 96-well plates at a density of 1×104 cells/well. Various concentrations of MXJDH were added and the cells were treated for 24 h. After CCK-8 reagent was added to each well for 1 h, the absorbance at
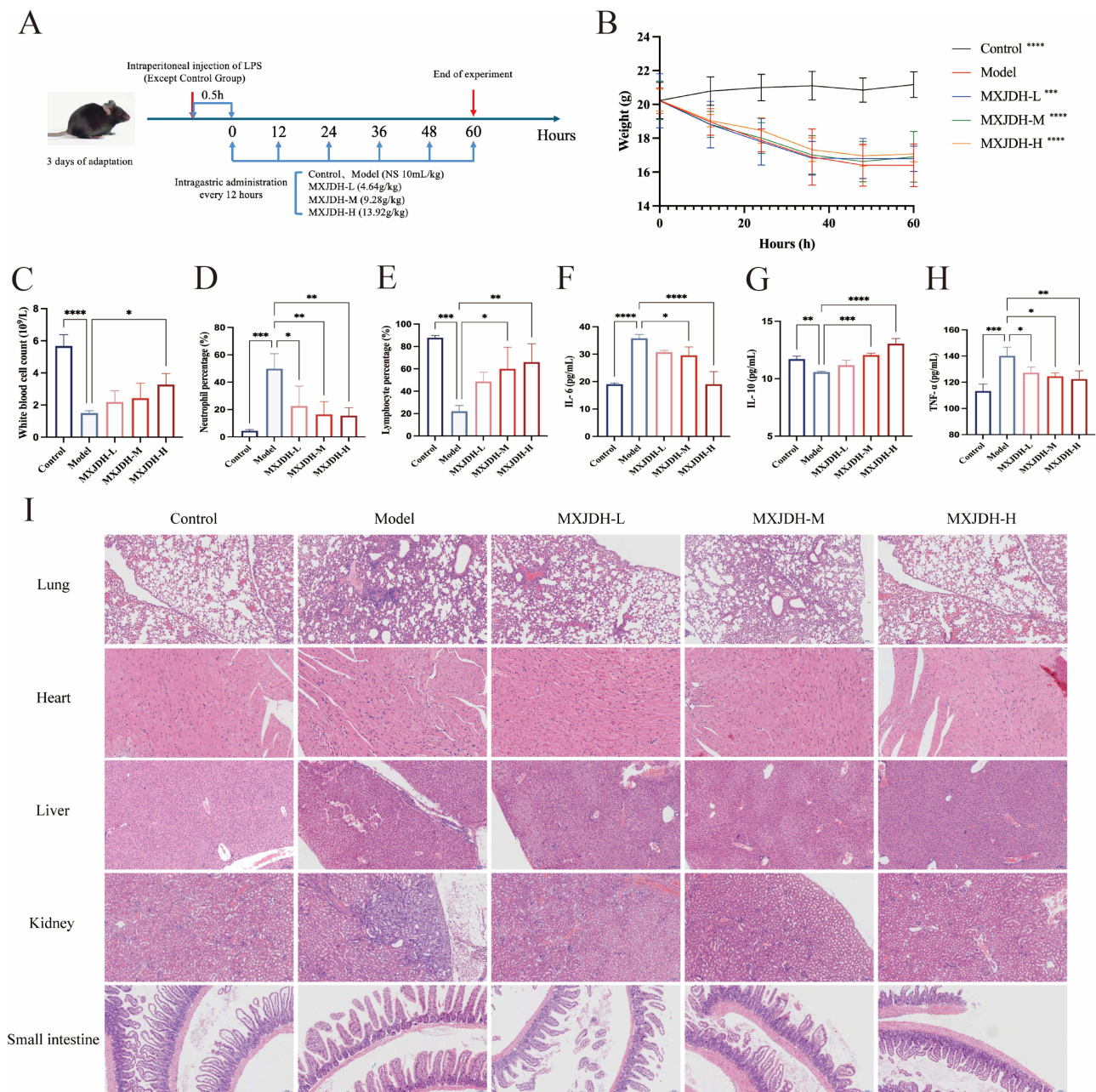
Figure 2 The effect of MXJDH on inflammatory states in sepsis mice. (**A**) Experimental design. (**B**) Weight of the mice (n = 6). (**C–E**) Effect of MXJDH on the white blood cell count, neutrophil percentage, and lymphocyte percentage of LPS-induced sepsis mice (n = 3). (**F–H**) Effect of MXJDH on inflammatory cytokines IL-6, IL-10 and TNF-α in serum of LPS-induced sepsis mice (n = 3). (**I**) Effect of MXJDH on five organs of lung, heart, liver, kidney and small intestine in mice with LPS-induced sepsis. Scale bars, 50 μm or 100 μm as indicated. Data were shown as mean ± SD and were analyzed using one-way ANOVA (nonparametric) analysis. *$P < 0.05$, **$p < 0.01$, ***$P < 0.001$, ****$P < 0.0001$, VS model group.

450 nm was measured using a Synergy HT Multimode Microplate Reader (BioTek, USA). 50, 100, and 150 μg/mL were selected for the subsequent experiments.

Transcriptome Sequencing

The control, model, and MXJDH-150μg/mL group cells were then sequenced. Total RNA was extracted from the cells using TRIzol reagent. The Applied Protein Technoligy (Shanghai, China) was used for RNA quality testing, cDNA library construction, library insert size, effective concentration detection, and sequencing. Based on these results,

subsequent quantitative analysis of gene expression, differential gene expression analysis, and functional enrichment analysis were performed.

Flow Cytometry Analysis

After washing the cells in PBS, CD86 was added and the cells were protected from light for 30 min. After washing in PBS, flow cytometry fixed buffer was added and the cells were fixed at room temperature in the dark for 20 min. Washed with Flow Cytometry Perm Buffer, and after centrifugation, resuspended the cells in Flow Cytometry Perm Buffer. CD206 was added for staining for 30 min. Washed 2 times, and then using a BD FACSCelesta flow cytometer (Shanghai, China).

Co-Immunoprecipitation (Co-IP)

According to the rProtein A/G IP/Co-IP Kit instructions, the magnetic beads were vortex and washed, then p65 antibody or IgG antibody was added and incubated at room temperature for 10 minutes. Added The lysed cell supernatant and incubated overnight at 4 °C. After washing, added SDS-PAGE Loading Buffer and heated at 95 °C for 5 min. The beads were discarded, and the supernatant was collected for SDS-PAGE.

Western Blot (WB)

Raw264.7 cells were lysed using RIPA Lysis buffer. Cytoplasmic and nuclear proteins were extracted using a Nuclear and Cytoplasmic Protein Extraction Kit, respectively. The protein concentration was measured using a BCA Protein Assay Kit. Proteins were separated by 8% or 12% sodium dodecyl sulfate-polyacrylamide gel electrophoresis and transferred to PVDF membranes. After incubation of the membrane with 5% skim milk powder solution for 2 h at room temperature, the membrane was washed three times with TBST and then incubated with primary antibody overnight. The membrane was washed thrice more with the corresponding secondary antibody for 1 h at room temperature and subsequently washed. Finally, the bands were analyzed using the ImageJ software after chemiluminescence detection.

Quantitative Reverse Transcription-Polymerase Chain Reaction (qRT-PCR)

Total RNA was extracted from the cells using a FastPure Complex Cell/Tissue Total RNA Isolation kit (Vazyme, China), extracted total RNA from RAW264.7 cells according to the manufacturer's instructions. RNA purity was quantified using an OD-1000+ Spectrophotometer (One Drop, China) for quality control purposes. All-in-One First-Strand Synthesis MasterMix (iScience, China) was used to convert the RNA into single-stranded cDNA. qRT-PCR was performed on a 7500 Real Time System (ThermoFisher, USA) using F488 SYBR qPCR Mix (iScience, China). The mRNA expression was analyzed and quantified using the 2-ΔΔCt method. Primer sequences are listed in Supplementary Table 3.

Cellular Immunofluorescence (IF)

The cells were fixed with 4% paraformaldehyde for 10 min, washed 3 times in PBST, and permeabilized with 0.2% Triton X-100 for 60 min. After blocking the cells with 5% FBS for 40 min, added p65 and pim2 antibodies and incubated overnight at 4 °C. Washed 3 times with PBST, fluorescent secondary antibodies were added and incubated on a shaker in the dark for 1 h. Joined DAPI. Localization was observed using an LSM-710 laser confocal microscope (Zmager Z2, Germany).

Organizational Immunofluorescence

Paraffin sections were dewaxed, fixed, and blocked, followed by the addition of F4/80, pim2, CD86 and CD206 antibodies. After blocking, the corresponding horseradish peroxidase-labelled secondary antibodies were added. The sections were then washed, DAPI was added, and the sections were sealed. The cells were observed under an LSM-710 laser confocal microscope (Zmager Z2, Germany).

Statistical Analysis

GraphPad Prism 10 was used to analyse all the data, and the data were shown as the mean ± standard error of the mean. One-way analysis of variance (ANOVA) was used to assess differences between groups, and was considered statistically significant when $p < 0.05$.

Results

MXJDH Increases Body Weight in Sepsis Mice

To observe the effect of MXJDH on the general condition of the mice, we recorded the change in body weight and mortality of the mice in each group. The results showed that MXJDH had no significant effect on mouse mortality but improved the body weight of the mice. No death occurred in any of the mice. After MXJDH treatment, the body weight of the model group decreased by 22.5% compared with that of the control group, whereas the body weight of the MXJDH-L group increased by 2.3% and 3.0% in the MXJDH-M group and 4.1% in the MXJDH-H group compared with the Model group. Figure 2B shows the changes in the body weight of the mice.

MXJDH Alleviates Inflammation Response in Sepsis Mice

We measured the white blood cell counts, neutrophil percentages, and lymphocyte percentages in mice to assess the degree of systemic inflammation. As shown in Figure 2C–E), compared with the control group, the neutrophil percentage in the model group was significantly increased, and the white blood cell counts and lymphocyte percentage were decreased, indicating that the modeling was successful. Compared to the model group, the inflammation response of mice in the MXJDH treatment groups was inhibited. Serum cytokine levels were also measured in the mice. As shown in Figure 2F–H), in comparison to the control group, the MXJDH-treated group demonstrated a decrease in the expression of pro-inflammatory cytokines such as IL-6 and TNF-α, and an increase in the expression of anti-inflammatory cytokines like IL-10 in mice with sepsis. These findings were dose-dependent, suggesting that MXJDH can promote the transition of macrophages from the pro-inflammatory M1 phenotype to the anti-inflammatory M2 phenotype.

MXJDH Protects the Organs of Sepsis Mice

The heart, lung, liver, kidney, and small intestine of mice were collected and stained with HE to observe the effects of MXJDH on the organs of mice. The results are shown in Figure 2I. Compared with the control group, the myocardial fibers in the model group were arranged in a chaotic and discontinuous manner. Pulmonary interstitial hyperemia, alveolar edema, hemorrhage, and numerous pink inflammatory exudates were observed in the pulmonary interstitium and alveolar cavity. Hepatocytes showed vacuolar degeneration, cytoplasmic shrinkage, and destruction of the normal structure of some hepatic lobules. Large areas of renal fibrosis and inflammatory tissue infiltration were observed in the kidneys, normal cell morphology was disrupted, and tubular shape was not obvious. Inflammatory cell infiltration was observed in the intestinal tissue; the pathological structure was severely damaged, and the hierarchy was unclear. After MXJDH treatment, organ damage in the mice in each group improved. Compared to the model group, the myocardial fibers of the MXJDH-H group were essentially orderly and coherent. There was little alveolar cavity exudation, and there was no obvious abnormality in the lung interstitium. The morphology of hepatocytes was normal, and the structure of the hepatic lobules was intact. The glomerular and tubular shapes were gradually regained, and the intestinal tissue structure was intact. These results indicated that MXJDH exerts a protective effect on the organs of mice with sepsis.

MXJDH Regulates the Expression of Pim2/NF-κB Pathway Genes

We initially performed cell viability assays (Figure 3A). To explore the mechanism of action of MXJDH in sepsis, transcriptome sequencing was performed. Figure 3B showed that the differences between the groups and the biological reproducibility of the samples within the groups were good. In total, 257 differentially expressed genes were identified in the 3 groups of samples (Figure 3C). Among these genes, we selected those that were upregulated in the Model group and downregulated in the MXJDH group by >4 times. Based on this criterion, we found that only Pim2 was associated with sepsis (Figure 3D–F). It has been confirmed that Pim2 is closely related to NF-κB.[7,14] The total expression of the
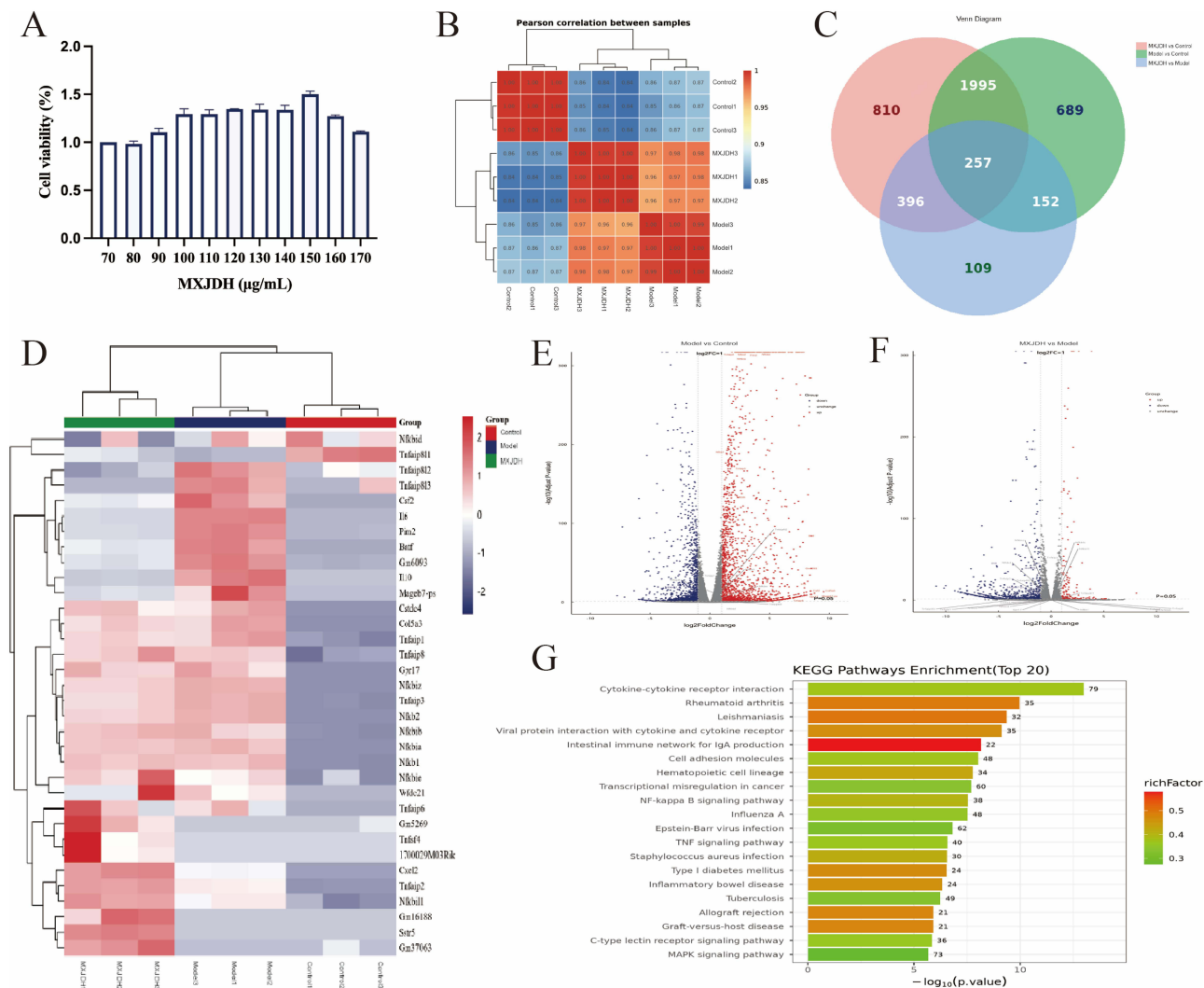
Figure 3 Cell viability and transcriptomic analysis of MXJDH. (**A**) Cell viability of different concentrations of MXJDH. (**B**) Heatmap of the correlation coefficient between samples. (**C**) Venn plots of differentially differentiated genes in different comparison groups. (**D**) Differential gene clustering map. (**E** and **F**) Volcano plot of differential gene expression distribution. (**G**) KEGG enrichment histogram of differentially expressed genes.

NF-κB signaling pathway was significantly increased in KEGG analysis (Figure 3G). Therefore, we hypothesized that MXJDH regulates downstream cytokine release, inhibits inflammatory responses, and ameliorates sepsis via the Pim2/NF-κB pathway. The alterations in NF-κB and downstream cytokines as depicted in the cluster plot and volcano plot validated our hypothesis.

MXJDH Regulates Macrophage Polarization

Macrophages can be polarized into two phenotypes, M1 pro-inflammatory and M2 anti-inflammatory, and play an important role in maintaining immune homeostasis.[15,16] Flow cytometry was used to determine the levels of M1 type surface molecular markers (CD86) and M2 type surface molecular markers (CD206) surface molecular markers in mouse macrophages. The results are shown in Figure 4A. We found that following LPS stimulation, there was a notable increase in the quantity of M1 macrophages. Upon treatment with MXJDH, a substance that requires further clarification, the count of M1 macrophages diminished, while the number of M2 macrophages saw a corresponding rise. This shift in macrophage types was found to be dependent on the concentration of the treatment, indicating a dose-responsive effect. These results suggest that MXJDH may regulate homeostasis of the internal environment by regulating macrophage polarization, thereby alleviating the inflammatory response.
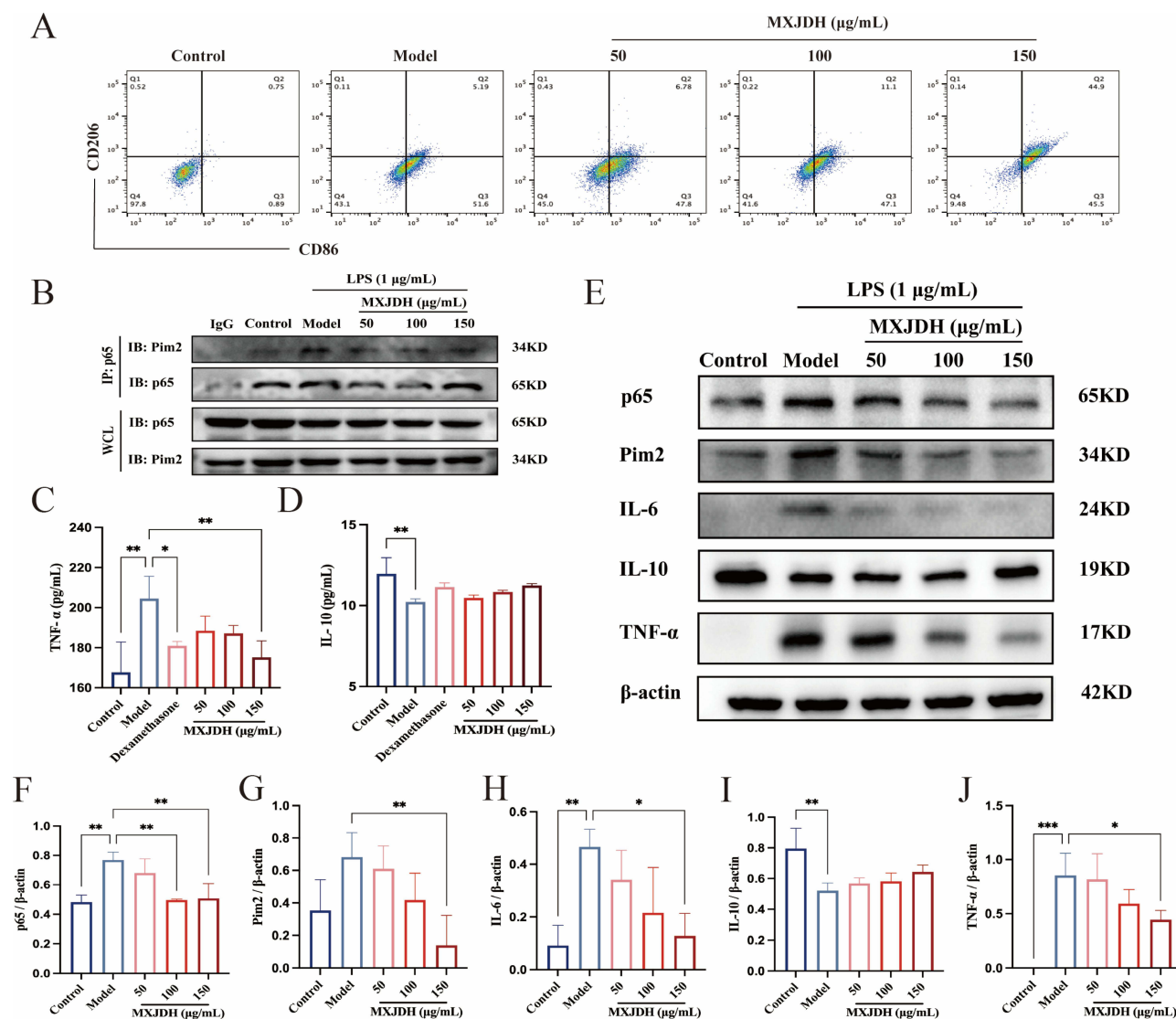
Figure 4 The effect of MXJDH on macrophage polarization and Pim2/NF-κB pathway. (**A**) Flow cytometry analysis of the effect of MXJDH on CD86 and CD206 expression in LPS-treated macrophages. (**B**) Co-IP analysis of the formation of Pim2-p65. (**C** and **D**) Effect of MXJDH and Dexamethasone on inflammatory cytokines TNF-α and IL-10 in LPS-treated macrophages (n=3). (**E**) Protein expression level of p65, Pim2, IL-6, IL-10 and TNF-α. (**F–J**) Statistical analysis of p65, Pim2, IL-6, IL-10 and TNF-α protein levels (n=3). Data were shown as mean ± SD and were analyzed using one-way ANOVA (nonparametric) analysis. *P < 0.05, **p <0.01, ***P < 0.001, VS model group.

MXJDH Attenuates Inflammation Response Through the Pim2/NF-κB Pathway

Based on the transcriptome analysis results, we speculated that MXJDH may mediate the inflammatory response through the Pim2/NF-κB pathway. Co-IP confirmed that Pim2 binds to NF-κB (Figure 4B). Additionally, compared to the dexamethasone treatment group, MXJDH therapy demonstrated a superior therapeutic effect. As shown in Figure 4C and D, both dexamethasone and MXJDH treatments could down-regulate the expression of TNF-α and up-regulate the expression of IL-10 compared to the model group. However, the therapeutic effect of MXJDH was significantly better than that of the dexamethasone group. To further explore the effect of MXJDH on related genes, we used Western blotting to detect the expression levels of IL-6, IL-10, and TNF-α in the Pim2/NF-κB signaling pathway in macrophages. As shown in Figure 4E–J, MXJDH treatment inhibited the expression of Pim2 and NF-κB, and all three concentrations decreased the expression of IL-6 and TNF-α, and increased the expression of IL-10. The high-dose group demonstrated the most significant therapeutic effect, with the medium-dose group showing a lesser degree of improvement. Next, we measured mRNA levels using qRT-PCR. The results shown in Figure 5A–E are consistent with the WB results. These results indicate that MXJDH inhibits NF-κB expression by regulating Pim2, thereby reducing the release of inflammatory cytokines and ameliorating sepsis. In order to
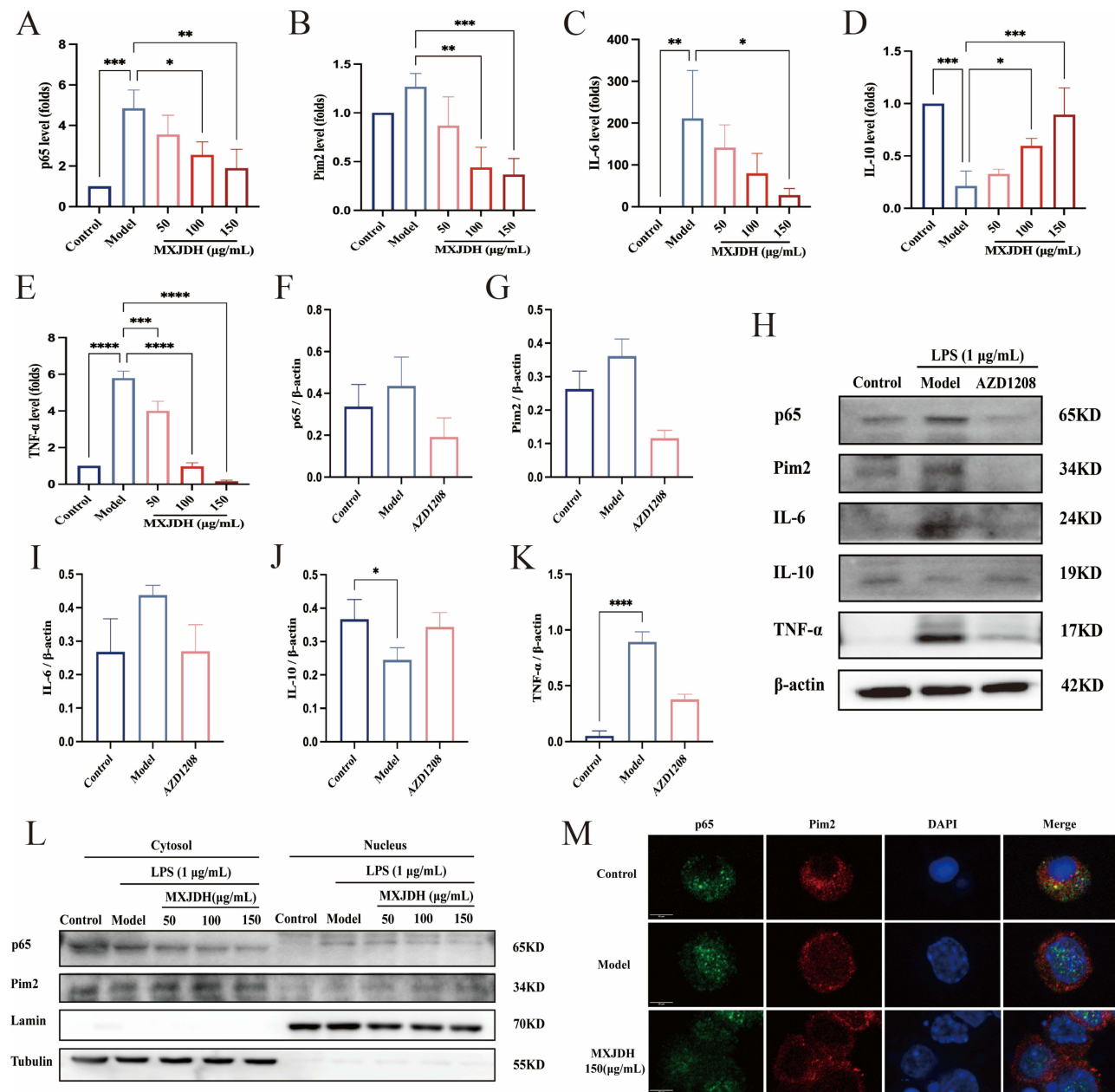
Figure 5 MXJDH ameliorates sepsis by inhibiting the Pim2/NF-κB pathway. (**A–E**) Statistical analysis of mRNA expression levels of p65, Pim2, IL-6, IL-10 and TNF-α (n=3). (**F–K**) Protein expression level of p65, Pim2, IL-6, IL-10 and TNF-α and statistical analysis (n=3). (**L**) Protein expression levels of p65 and Pim2 in cytoplasm and nucleus. (**M**) Representative images of P65, Pim2 immunofluorescence staining, and nuclear staining by DAPI. Scale bars, 20 μm as indicated. Data were shown as mean ± SD and were analyzed using one-way ANOVA (nonparametric) analysis. *P < 0.05, **p <0.01, ***P < 0.001, ****P < 0.0001, VS model group.

investigate if the Pim2/NF-κB pathway is the main target of MXJDH, we treated macrophages activated by LPS with the Pim2 inhibitor AZD1208. The findings, presented in Figure 5F–K, demonstrate that AZD1208 significantly reduces the production of p65 and subsequent pro-inflammatory factors, while enhancing the production of anti-inflammatory factors. To clarify the site of the interaction between Pim2 and NF-κB, we also detected IF, cytoplasmic, and nuclear proteins and found that after LPS stimulation, Pim2 almost did not enter the nucleus, NF-κB entered the nucleus in large quantities, and NF-κB nuclear entry was significantly reduced after MXJDH treatment (Figure 5L and M). These results suggest that Pim2 may induce nuclear ectopy in NF-κB by interacting with NF-κB in the cytoplasm, stimulating the release of downstream pro-inflammatory factors, facilitating the conversion of macrophages to the M1 phenotype, and developing cytokine release syndrome (CRS),
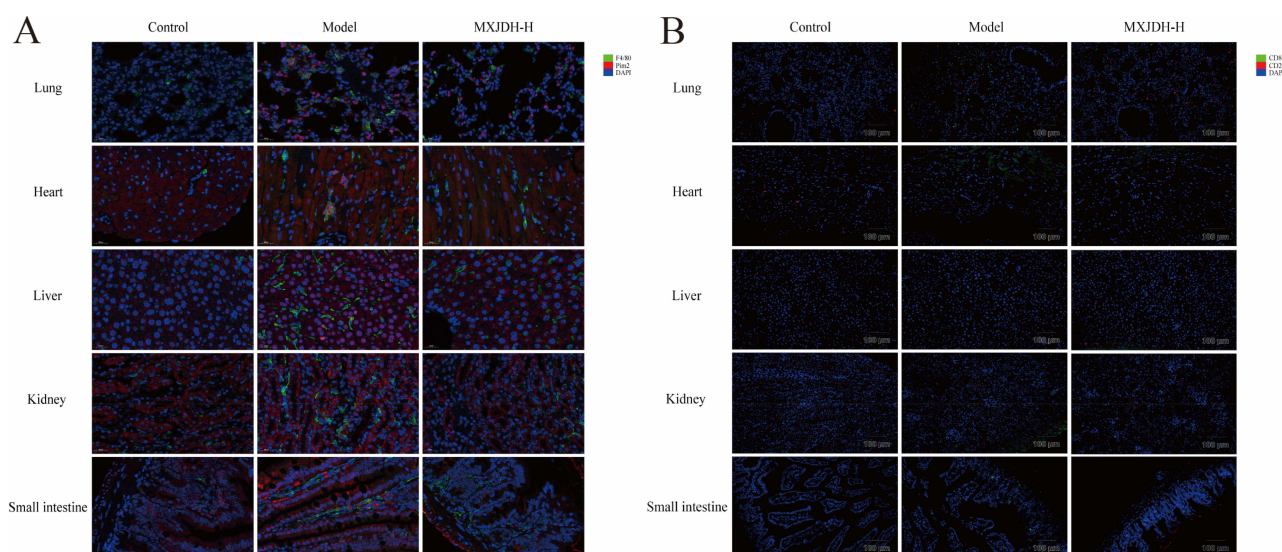
Figure 6 The effect of MXJDH on macrophages in sepsis mice. (**A**) Representative images of F4/80, Pim2 immunofluorescence staining, and nuclear staining by DAPI. Scale bars, 25 μm as indicated. (**B**) Representative images of CD86, CD206 immunofluorescence staining, and nuclear staining by DAPI. Scale bars, 100 μm as indicated.

leading to the occurrence of sepsis. However, MXJDH inhibited the expression of Pim2, reduced the nuclear translocation of NF-κB, influenced macrophage polarization, and ameliorated sepsis.

MXJDH Reduces the Expression of pim2 in Macrophages of Sepsis Mice

We performed immunofluorescence staining of the heart, lungs, liver, kidneys, and small intestine of mice. As shown in Figure 6A, the expression of F4/80 and Pim2 in mouse macrophages increased after LPS stimulation. Both expression levels were reduced compared to those in the model group. These results suggest that MXJDH attenuates the inflammatory response and reduce the expression of pim2 in macrophages. Subsequently, to further investigate the effect of MXJDH on the polarization process of macrophages in septic mice, we conducted tissue immunofluorescence staining for two markers, CD86 and CD206. The results (as shown in Figure 6B) indicate that in the sepsis model group of mice, the expression of M1 macrophage markers significantly increased. After MXJDH treatment, the expression of M1 macrophage markers decreased, while the expression of M2 macrophage markers correspondingly increased. This phenomenon suggests that MXJDH may promote the transformation of macrophages from the pro-inflammatory M1 type to the anti-inflammatory M2 type.

Discussion

Sepsis is the leading cause of infection death worldwide.[17] Studies have shown that the levels of serum interleukin-1β (IL-1β), IL-2, IL-7, tumor necrosis factor-α (TNF-α) and other pro-inflammatory factors in patients with sepsis are significantly increased, and this CRS, which significantly increases case fatality rate, is the main cause of multiple organ dysfunction such as acute respiratory distress syndrome. Many studies have attempted to treat CRS inhibition; however, there has been no effective clinical progress.[18,19]

Most macrophages are monocytic. Monocytes are released from the bone marrow, circulate in various body tissues, and differentiate into mature macrophages. These mature macrophages, in response to different environmental stimuli, can differentiate into two phenotypes, M1 and M2.[20,21] M1 macrophages are mainly induced by LPS and interferon-γ (IFN-γ) and secrete a large number of pro-inflammatory factors, such as IL-1β and TNF-α; therefore, they are also called pro-inflammatory macrophages. M2 macrophages have a strong phagocytic ability and are known as anti-inflammatory macrophages, mainly producing anti-inflammatory factors, such as IL-10 and transforming growth factor-β (TGF-β).[22,23] Regulation of macrophage immune metabolism, especially inhibition of CRS, is a feasible direction for the treatment of inflammatory diseases.

Proviral integration site 2 (Pim2), which exhibits serine/threonine kinase activity, is a protein coding gene. It is involved in cell survival and proliferation, and is closely associated with tumor diseases of the immune, reproductive, and other systems.[5,6,14] Additionally, Pim2 is closely related to inflammation. Overexpression of Pim2 enhances the expression of IL-6, IL-1β, and TNF-α. However, the expression of IL-6 was significantly reduced after the stimulation of Pim2 gene-deficient mice with LPS.[24] Recent studies have shown that pim2 is involved in NF-κB-related pathways through which cytokine expression is regulated, thus affecting the inflammatory response.[7,25,26] The NF-κB pathway is a well-established pro-inflammatory signaling pathway that mediates the inflammatory response by regulating pro-inflammatory cytokine production, leukocyte recruitment, or cell survival. There are two main ways to activate this pathway: canonical and non-canonical NF-κB signalling pathways. The former releases NF-kB dimers by degrading IκB proteins and the latter activates NF-κB by converting p100 to p52, both of which ultimately facilitate the transfer of NF-κB from the cytoplasm to the nucleus, which in turn mediates downstream reactions.[27–29] Pim2 can mediate NF-kB ectopy by regulating the phosphorylation of enzymes, thereby activating the NF-kB signaling pathway.[7,14] However, existing research on the Pim2/NF-κB pathway has mainly focused on tumors, and there is a lack of research on inflammation.

This study reports the therapeutic effects of MXJDH in mice with sepsis and elucidates its possible mechanism of action. We found that MXJDH, through the synergistic effect of its multiple components, improved the general state of mice and had a protective effect on organs by alleviating sepsis-induced multi-organ dysfunction. Additionally, we found that MXJDH played a role in immune regulation. After MXJDH treatment, macrophages gradually transformed from M1 to M2, the release of pro-inflammatory cytokines decreased, anti-inflammatory cytokines increased, and CRS was inhibited, thereby alleviating the inflammatory response. Mechanistically, Pim2, recognized as a highly promising therapeutic target, is not only involved in tumor-related diseases but also plays a crucial role in the progress of inflammation. The Pim2/NF-κB signaling pathway is involved in MXJDH-mediated improvement of sepsis. Pim2 controls the movement of NF-κB into the nucleus, which triggers the release of pro-inflammatory cytokines, leading to the polarization of macrophages towards the M1 type. Inhibiting Pim2 decreases the production of pro-inflammatory cytokines and increases the production of anti-inflammatory factors, thereby polarizing macrophages towards the M2 type. MXJDH can modulate the expression of Pim2 and decrease its interaction with NF-κB in the cytoplasm. This action reduces NF-κB entry into the nucleus, modulating the secretion of downstream inflammatory cytokines, and promoting the conversion of macrophages from the M1 to the M2 type, ultimately aiming to improve sepsis.

There is a limited understanding of the Pim2/NF-κB pathway in the context of inflammation, and the research on how traditional Chinese medicine can modulate this pathway is also sparse. Our research has elucidated how MXJDH influences the polarization of macrophages and enhances the recovery from sepsis through its effects on the Pim2/NF-κB pathway. However, this study has some limitations. First, the scope of our research is limited, and it does not rule out the possibility that MXJDH may regulate sepsis through signaling pathways other than Pim2/NF-κB. Second, this study believed that pim2 activated the classical pathway of NF-κB, but phosphorylation and IκB protein tests were not performed. The involvement of non-classical pathways could not be ruled out, and the evidence chain was incomplete. Third, in the study of macrophage polarization, owing to the small collection of macrophages in the peritoneal cavity of mice, only in vitro experiments were performed, and in vivo double validation was lacking. Fourth, the current research is primarily concentrated on macrophages, without investigating the possible effects of MXJDH on other immune cells. Fifth, the research lacks a thorough investigation into clinical translational challenges, including the establishment of standardized dosing regimens and the potential adverse effects or toxicity profiles of the drug.

Conclusion

The clinical efficacy of MXJDH in the treatment of sepsis is clear, but mechanistic research is still lacking. The results of this study suggest that MXJDH may alleviate inflammation and sepsis by regulating macrophage polarization and inhibiting the Pim2/NF-κB pathway, thus providing a theoretical basis for the clinical treatment of sepsis.

Ethics Statement

All animal studies were performed in accordance with the guidelines and regulations for the use and care of animals at the Centre for Laboratory Animal Care, Nanjing University of Chinese Medicine.

Acknowledgments

Disclosure

The authors report no conflicts of interest in this work.

References

1. Liu D, Huang SY, Sun JH, et al. Sepsis-induced immunosuppression: mechanisms, diagnosis and current treatment options. *Mil Med Res*. 2022;9 (1):56. In eng. doi:10.1186/s40779-022-00422-y
2. Evans T. Diagnosis and management of sepsis. *Clin Med*. 2018;18(2):146–149. In eng. doi:10.7861/clinmedicine.18-2-146
3. Huang M, Cai S, Su J. The pathogenesis of sepsis and potential therapeutic targets. *Int J Mol Sci*. 2019;20(21). In eng. doi:10.3390/ijms20215376
4. Vincent JL. Current sepsis therapeutics. *EBioMedicine*. 2022;86:104318. In eng. doi:10.1016/j.ebiom.2022.104318
5. Liu Z, Guo Y, Liu X, et al. Pim-2 kinase regulates energy metabolism in multiple myeloma. *Cancers*. 2022;15(1). doi:10.3390/cancers15010067
6. Lu C, Qiao P, Fu R, et al. Phosphorylation of PFKFB4 by PIM2 promotes anaerobic glycolysis and cell proliferation in endometriosis. *Cell Death Dis*. 2022;13(9):790. In eng. doi:10.1038/s41419-022-05241-6
7. Tang X, Cao T, Zhu Y, et al. PIM2 promotes hepatocellular carcinoma tumorigenesis and progression through activating NF-κB signaling pathway. *Cell Death Dis*. 2020;11(7):510. In eng. doi:10.1038/s41419-020-2700-0
8. Tang Q, Tang Y, Yang Q, et al. Embelin attenuates lipopolysaccharide-induced acute kidney injury through the inhibition of M1 macrophage activation and NF-κB signaling in mice. *Heliyon*. 2023;9(3):e14006. In eng. doi:10.1016/j.heliyon.2023.e14006
9. Xiong Y, Zhang Z, Liu S, et al. Lupeol alleviates autoimmune myocarditis by suppressing macrophage pyroptosis and polarization via PPARα/ LACC1/NF-κB signaling pathway. *Phytomedicine*. 2024;123:155193. In eng. doi:10.1016/j.phymed.2023.155193
10. Luo P, Zhang Q, Zhong TY, et al. Celastrol mitigates inflammation in sepsis by inhibiting the PKM2-dependent Warburg effect. *Mil Med Res*. 2022;9(1):22. In eng. doi:10.1186/s40779-022-00381-4
11. Yang X, Lu L, Wu C, Zhang F. ATP2B1-AS1 exacerbates sepsis-induced cell apoptosis and inflammation by regulating miR-23a-3p/TLR4 axis. *Allergol Immunopathol*. 2023;51(2):17–26. doi:10.15586/aei.v51i2.782
12. Liu H, Zhou L, Wang X, et al. Dexamethasone upregulates macrophage PIEZO1 via SGK1, suppressing inflammation and increasing ROS and apoptosis. *Biochem Pharmacol*. 2024;222:116050. doi:10.1016/j.bcp.2024.116050
13. Katsuta E, Gil-Moore M, Moore J, et al. Targeting PIM2 by JP11646 results in significant antitumor effects in solid tumors. *Int J Oncol*. 2022;61 (4). doi:10.3892/ijo.2022.5404
14. Wang JC, Chen DP, Lu SX, et al. PIM2 expression induced by proinflammatory macrophages suppresses immunotherapy efficacy in hepatocellular carcinoma. *Cancer Res*. 2022;82(18):3307–3320. In eng. doi:10.1158/0008-5472.Can-21-3899
15. Cutolo M, Campitiello R, Gotelli E, Soldano S. The role of M1/M2 macrophage polarization in rheumatoid arthritis synovitis. *Front Immunol*. 2022;13:867260. In eng. doi:10.3389/fimmu.2022.867260
16. Wang C, Ma C, Gong L, et al. Macrophage polarization and its role in liver disease. *Front Immunol*. 2021;12:803037. In eng. doi:10.3389/ fimmu.2021.803037
17. Gauer R, Forbes D, Boyer N. Sepsis: diagnosis and management. *Am Fam Physician*. 2020;101(7):409–418. In eng.
18. Huang C, Wang Y, Li X, et al. Clinical features of patients infected with 2019 novel coronavirus in Wuhan, China. *Lancet*. 2020;395 (10223):497–506. In eng. doi:10.1016/s0140-6736(20)30183-5
19. Cecconi M, Evans L, Levy M, Rhodes A. Sepsis and septic shock. *Lancet*. 2018;392(10141):75–87. In eng. doi:10.1016/s0140-6736(18)30696-2
20. Boutilier AJ, Elsawa SF. Macrophage polarization states in the tumor microenvironment. *Int J Mol Sci*. 2021;22(13):6995. In eng. doi:10.3390/ ijms22136995
21. Chen X, Liu Y, Gao Y, Shou S, Chai Y. The roles of macrophage polarization in the host immune response to sepsis. *Int Immunopharmacol*. 2021;96:107791. In eng. doi:10.1016/j.intimp.2021.107791
22. Gauthier T, Chen W. Modulation of macrophage immunometabolism: a new approach to fight infections. *Front Immunol*. 2022;13:780839. In eng. doi:10.3389/fimmu.2022.780839
23. Kadomoto S, Izumi K, Mizokami A. Macrophage Polarity and Disease Control. *Int J Mol Sci*. 2021;23(1):144. In eng. doi:10.3390/ijms23010144
24. Yang J, Li X, Hanidu A, et al. Proviral integration site 2 is required for interleukin-6 expression induced by interleukin-1, tumour necrosis factor-α and lipopolysaccharide. *Immunology*. 2010;131(2):174–182. In eng. doi:10.1111/j.1365-2567.2010.03286.x
25. Lu C, Ren C, Yang T, et al. Fructose-1, 6-bisphosphatase 1 interacts with NF-kappaB p65 to regulate breast tumorigenesis via PIM2 induced phosphorylation. *Theranostics*. 2020;10(19):8606–8618. doi:10.7150/thno.46861
26. Wang F, Xu L, Dong G, Zhu M, Liu L, Wang B. PIM2 deletion alleviates lipopolysaccharide (LPS)-induced respiratory distress syndrome (ARDS) by suppressing NLRP3 inflammasome. *Biochem Biophys Res Commun*. 2020;533(4):1419–1426. doi:10.1016/j.bbrc.2020.08.109
27. Sun SC. The non-canonical NF-κB pathway in immunity and inflammation. *Nat Rev Immunol*. 2017;17(9):545–558. In eng. doi:10.1038/ nri.2017.52
28. Xiao Z, Kong B, Fang J, et al. Ferrostatin-1 alleviates lipopolysaccharide-induced cardiac dysfunction. *Bioengineered*. 2021;12(2):9367–9376. In eng. doi:10.1080/21655979.2021.2001913
29. Fung SY, Lu HY, Sharma M, et al. MALT1-dependent cleavage of HOIL1 modulates canonical NF-κB signaling and inflammatory responsiveness. *Front Immunol*. 2021;12:749794. In eng. doi:10.3389/fimmu.2021.749794